Environmental Technology & Innovation 30 (2023) 103138

Contents lists available at ScienceDirect

Environmental Technology & Innovation

journal homepage: www.elsevier.com/locate/eti

Adsorption–desorption behavior of malachite green by potassium permanganate pre-oxidation polyvinyl chloride microplastics

Kefu Wang [a], Kangkang Wang [a], Yaoyao Chen [a], Siqi Liang [a], Changyan Guo [a], Wei Wang [b,c,*], Jide Wang [a,*]

[a] Key Laboratory of Oil and Gas Fine Chemicals, Ministry of Education & Xinjiang Uygur Autonomous Region, School of chemical engineering and technology, Xinjiang University, Urumqi, China
[b] Department of Chemistry, University of Bergen, Bergen 5007, Norway
[c] Center for Pharmacy, University of Bergen, Bergen 5020, Norway

ARTICLE INFO

Article history:
Received 12 February 2023
Received in revised form 23 March 2023
Accepted 4 April 2023
Available online 10 April 2023

Keywords:
Malachite green
Polyvinyl chloride microplastics
Pre-oxidation
Adsorption and desorption
Simulated gastrointestinal fluids

ABSTRACT

Microplastics (MPs) and the typical hydrophilic organic pollutant Malachite green (MG) are frequently detected in sewage treatment plants. Potassium permanganate ($KMnO_4$) pre-oxidation is an economical and effective technology in wastewater treatment. It is important to study the surface physicochemical characteristics of MPs and understand their fate in wastewater treatment plants after pre-oxidation. In this study, Polyvinyl chloride (PVC) MPs were treated by single and composite $KMnO_4$ pre-oxidation with different pH values. After the pre-oxidation treatment, the appearance of O–Mn spectra and surface nanoparticles indicated the oxides (MnO_2) were produced on the MPs surface. Moreover, the adhesion of MnO_2 is helpful to improve the hydrophilicity and adsorption capacity of MG. The adsorption capacity of pristine PVC for MG was 2.6 mg/g. But the adsorption capacity increased to 7.0 mg/g for single oxidation and 140.7 mg/g for composite oxidation, respectively. The desorption experiment results indicate the pre-oxidation process could reduce the release efficiency of MG from the PVC MPs due to the better binding of surface MnO_2 nanoparticles to MG. However, the total desorption capacity is still high. which illustrates that there is a high potential risk of MG which can transfer from the surface of the PVC MPs to the gastrointestinal fluids.

1. Introduction

Microplastics (MPs), commonly defined as plastic particles with an effective diameter of less than 5 mm (Li et al., 2018), can enter the ecosystem through various pathways (Bhagat et al., 2021; Payton et al., 2020; Sussarellu et al., 2016). They are either suspended in the water column or deposited on the bottom, and studies have shown that they are widespread in marine ecosystems and freshwater ecosystems such as rivers (Wang et al., 2020), lakes (Egessa et al., 2020), soil (Steinmetz et al., 2016), sediment (Fu et al., 2020; Nuelle et al., 2014), polar environments (Kelly et al., 2020) and even in drinking water (Jian et al., 2020). MPs have the characteristics of small size, large specific surface area and highly hydrophobic, which makes it easy to adsorb heavy metals (Huffer et al., 2018), organic pollutants (Bakir et al., 2014) and disease-causing

* Corresponding authors.
E-mail addresses: gcyslw@xju.edu.cn (C. Guo), wei.wang@uib.no (W. Wang), awangjd@sina.cn (J. Wang).

https://doi.org/10.1016/j.eti.2023.103138

microorganisms (Guo et al., 2019). MPs adsorbed pollutants can not only cause physical damage to organisms through feeding but also release toxic and harmful pollutants, resulting in direct or indirect toxicological effects on the ecosystem (Dong et al., 2021), thus potentially endangering the safety of marine, freshwater and soil ecosystems (Jin et al., 2018). Wastewater treatment plants often contain a large number of MPs, but the current treatment process does not specifically have technologies for MPs removal (Freeman et al., 2020; Leslie et al., 2017). Although conventional treatment methods can remove most MPs, MPs in small sizes are still discharged into the natural environment with the effluent of sewage treatment plants (Jiang et al., 2020; Rolsky et al., 2020; Zhang and Chen, 2020). As a result, more attention has been paid to the potential ecological health risks of MPs from wastewater treatment plants.

MPs are inevitably exposed to the environment, and various environmental factors will cause chemical changes on their surface, such as the increase of specific surface area, oxygen-containing functional groups and hydrophilicity, which will affect the sorption and desorption capacity of MPs to environmental pollutants. Therefore, a large number of studies are still needed to confirm how aging affects the physicochemical properties of MPs and their subsequent adsorption–desorption behavior to pollutants in the aqueous environment. At present, the simulated aging conditions are limited, and various artificial accelerated aging conditions are generally used to treat MPs in the laboratory, including Fenton and thermally activated $K_2S_2O_8$ techniques (Liu et al., 2019), UV irradiation in air/simulated seawater/H_2O_2 (Cai et al., 2018; Huffer et al., 2018), O_3 exposure and freeze-thaw cycle aging, and high-temperature oxidation aging (Sun et al., 2022). However, pre-oxidation disinfection processes are widely used in water and wastewater treatment plants, including membrane separation, flotation, biodegradation, biological enzyme, photocatalytic degradation, and coagulation sedimentation (Ahmed et al., 2022). The purpose of these pre-oxidation methods is to inactivate algae/cyanobacteria (Li et al., 2014) and degrade organic matter (Lin et al., 2020a, 2020b). Wastewater treatment technology has a certain effect on the removal of MPs, and the potassium permanganate ($KMnO_4$) was proved to have the potential to affect the physical and chemical properties of MPs due to the strong oxidizing property. It is important to reveal the changes in the surface physicochemical characteristics of MPs and the mechanism during the chemical pre-oxidation process. This change may affect the interaction between MPs with other pollutants, thus affecting the carrier effect of MPs and the adsorption–desorption behavior of pollutants. However, the effects of these chemical pre-oxidation methods on MPs have been poorly studied, so related studies deserve further attention.

MPs are small in size and easily ingested by aquatic organisms, causing irreversible damage to their liver and stomach (Coffin et al., 2019a,b; Guo et al., 2020). After MPs enter the gastrointestinal environment of organisms, the MPs adsorbed by toxic substances may be released and affect the normal life activities of organisms. The issue of malachite green (MG) contamination in the environment has been of great concern, which is often used in paper, wood, silk and leather, and can cause multiple toxic risks to humans (Crini, 2006; Ferreira et al., 2014). Moreover, MPs and MG may coexist in large quantities in aquatic environments, so it is essential to study the interaction between MPs and MG. Unlike the aqueous environment, composite biological conditions in living organisms may enhance the potential effects of MPs. Studies have shown that MPs entering the gastrointestinal fluids of organisms from the aqueous body will stay in the gastrointestinal tract (GIT) system consisting of the stomach, small intestine and large intestine regions (Jeong et al., 2016). Moreover, the contaminants loaded on the surface of MPs will also undergo a degree of desorption in the GIT system, and the desorption of contaminants in the GIT environment is higher than that in natural water (Godoy et al., 2020; Holmes et al., 2020; Liao and Yang, 2020). Therefore, further studies focusing on the desorption of MG-loaded MPs in gastrointestinal fluids are necessary.

Herein, the effects of $KMnO_4$ single oxidation and UV/$KMnO_4$ composite oxidation on the environmental behavior of MPs were investigated. PVC MPs were selected as representative MPs because they were often detected in real water environments and wastewater treatment effluents. The objectives of this study include: (1) investigating the changes in morphology, surface property and hydrophobicity of PVC MPs during $KMnO_4$ pre-oxidation; (2) exploring the adsorption behavior of MG on pristine and pre-oxidation PVC MPs, including adsorption kinetics, adsorption isotherms, and the effect of environmental conditions salinity and pH; (3) studying the desorption behavior of MG-loaded PVC MPs in ultrapure water, seawater, and simulated cold-blooded and warm-blooded organisms under intestinal and gastric fluids; (4) investigating the adsorption mechanism of MG on pristine and pre-oxidation PVC MPs.

2. Material and methods

2.1. Materials

The materials were described in Section 1.1 in Supporting Information (SI).

2.2. Characterization of MPs

The characterization was described in Section 1.2 in SI.

2.3. $KMnO_4$ pre-oxidation experiments

The reaction of $KMnO_4$ oxidation was conducted in 50 mL brown glass vials with threaded lids. $KMnO_4$ solutions with given concentrations were prepared with pH adjustment using H_2SO_4 solution (1%) and NaOH solution (0.1 mol/L). In actual sewage treatment, typically 0.4–10 mg/L $KMnO_4$ oxidation was applied (Lin et al., 2013). To obtain evident effects of $KMnO_4$ oxidation on MPs, the concentration at 10 mg/L was selected. In each reaction system, 40 mL of solution was added, then 2 g PVC MPs were added subsequently. Then placed in a constant temperature water bath shaker at 160 rpm at 25 °C for 12 h and UV aging chamber for 12 h. UV aging experiments were carried out in an aging chamber with a UVA-340 lamp (Q-Lab Corporation) at 25 °C. Sampling was conducted by filtering the suspension using 0.22 μm hydrophilic polytetrafluoroethylene (PTFE) filters. The separated PVC MPs particles were washed with ultrapure water and dried at 40 °C overnight. And then the PVC MPs were characterized, named as pH = 3 PVC, pH = 7 PVC, pH = 11 PVC, pH = 3+UV PVC, pH = 7+UV PVC and pH = 11+UV PVC, respectively.

2.4. Adsorption experiments

All adsorption experiments were carried out with brown glass bottles in triplicate to minimize experimental errors. Meanwhile, the blank experiments were conducted under the same conditions as all adsorption experiments to ensure experimental accuracy.

In the kinetics experiment, 200 mg of pristine PVC MPs, 100 mg of single oxidation PVC MPs and 5 mg composite oxidation PVC MPs were added into 50 mL brown glass vials with threaded lids containing 40 mL of 20 mg/L MG, then the vials were shaken in the dark at 25 °C in a thermostatic shaker at 160 rpm. These concentration ranges were determined from a preliminary experiment to guarantee a 20%–80% uptake of the sorbates at equilibrium. The adsorption capacity was assessed at time intervals of 0.5, 1, 2, 4, 8, 12, 24, 48, 60 and 72 h. The kinetics data showed sorption equilibrium of MG on MPs was achieved within 60 h, so 60 h was adopted for subsequent adsorption tests. For the sorption isotherm experiments, the MG solutions with different concentrations (5, 10, 15, 20, 30, 40, and 50 mg/L) were added to the brown glass vials. The samples were shaken at 160 rpm for 60 h to achieve equilibrium. To examine the effect of pH and salinity, the pH was adjusted in the range of 3–7 with 0.1 mol/L HCl and NaOH; the salinities were adjusted to 5–50‰ using NaCl. The initial concentrations of MG solutions were 20 mg/L, and all the samples were shaken at 160 rpm for 60 h. All collected samples were passed through 0.22 μm filters to remove PVC MPs.

2.5. Desorption experiments in simulated gastric and intestinal conditions

The MG-loaded pristine and pre-oxidation PVC MPs were prepared by spiking 20 mg/L MG into 50 mL brown glass vials containing a certain amount of pristine and pre-oxidation PVC MPs. The mixture was shaken at 160 rpm for 60 h to reach sorption equilibrium according to the sorption kinetics experiment. After sorption equilibrium, the PVC MPs were collected via vacuum filtration, washed three times with ultrapure water, and then air dried for 48 h. Desorption experiments were studied in ultrapure water (pH = 7.2), simulated seawater, gastric fluid (pH = 2) and intestinal fluid (pH = 7). Simulated gastric fluid was prepared by adding pepsin in 100 mmol/L of NaCl solution to a final concentration of 3.2 g/L. Simulated intestinal fluid consisted of 5.0 g/L BSA and 10 mmol/L NaT in 100 mmol/L NaCl solution (Lee et al., 2019; Mohamed Nor and Koelmans, 2019). The pH of gastric and intestinal fluids was adjusted to 2.0 and 7.0, respectively to mimic the acidic stomach and neutral gut environments. Simulated seawater (550 mmol/L NaCl and pH 7.0) was prepared for comparison (Coffin et al., 2019b). For desorption kinetic experiments, 40 mL gastrointestinal fluids were spiked into a vial containing 200 mg of pristine PVC MPs, 100 mg of single oxidation PVC MPs and 5 mg composite oxidation PVC MPs loaded MG, respectively. and then was incubated in a rotary shaker at 160 rpm for 72 h. The temperature was kept at 18 °C and 37 °C to mimic the gastrointestinal fluids of cold- and warm-blooded marine organisms, respectively (Tanaka et al., 2015).

2.6. Data analysis/statistics

The detailed information on the method was given in Section 1.3 in SI.

3. Results and discussion

3.1. Surface chemical variations

3.1.1. The characterization of PVC MPs

To analyze the effects of pre-oxidation and to understand the changes of functional groups on the surface of PVC MPs, the infrared spectra of PVC MPs were scanned as shown in Fig. S1a. From the infrared spectra of PVC MPs pre-oxidation with $KMnO_4$ at different pH values can be seen that there are no new absorption bands were generated, indicating that no new functional groups were formed on the surface of PVC MPs after oxidation. This result can also be confirmed by the surface change result of PVC MPs after UV/$KMnO_4$ composite oxidation shown in Fig. S1b. According to the result,

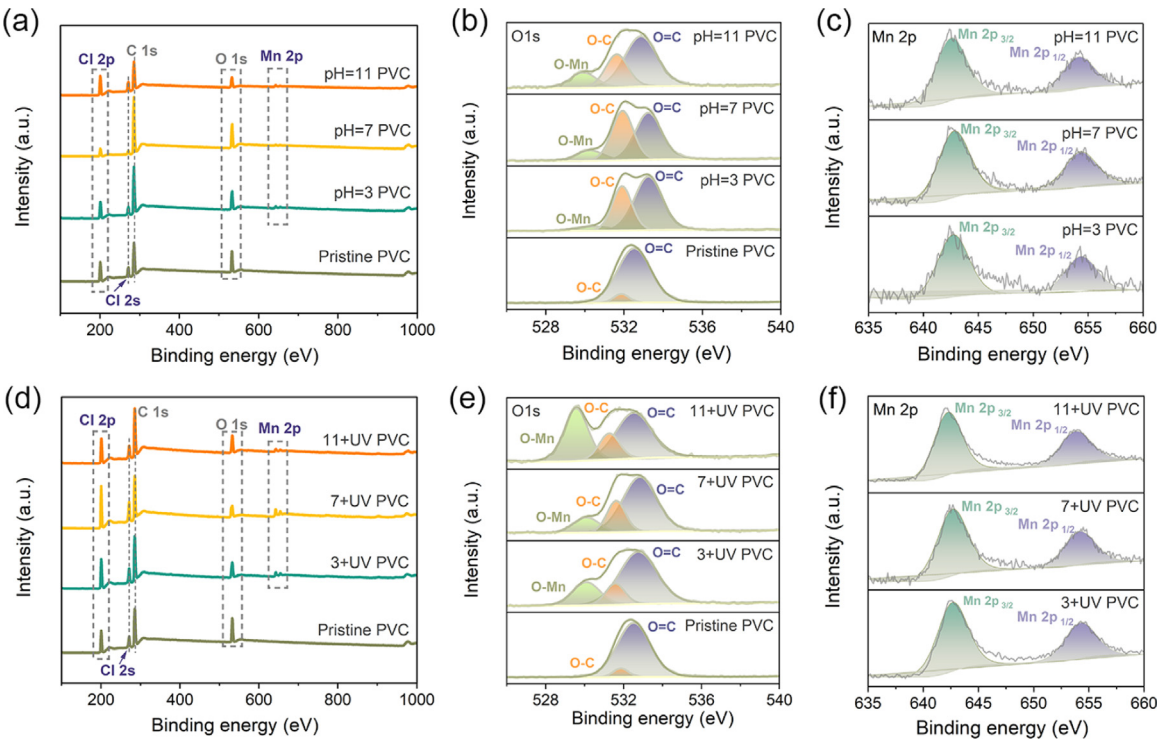

Fig. 1. X-ray photoelectron spectroscopy variations of PVC MPs. (a) Survey spectrum of pristine and single oxidation PVC MPs under pH = 3, 7, 11; (b) O 1s spectrum of pristine and single oxidation PVC MPs; (c) Mn 2p spectrum of single oxidation PVC MPs; (d) Survey spectrum of pristine and composite oxidation PVC MPs; (e) O 1s spectrum of pristine and composite oxidation PVC MPs; (f) Mn 2p spectrum of composite oxidation PVC MPs;.

the infrared spectrum changes were relatively small after composite oxidation, which may be mainly due to the short oxidation time. The specific surface area of aged MPs increased and new functional groups were formed after 24 days of UV aging (Li et al., 2022). The photoaging properties and mechanism of PVC MPs under different UV irradiation in air or water, they found that with the increase of aging time, the oxygen-containing functional groups, carbonyl index higher and crystallinity of aged PVC increased (Ouyang et al., 2022). In general, the insignificant change in FTIR curves indicated that $KMnO_4$ pre-oxidation had a limited effect on the PVC MPs surface. We have further used XRD characterization tests to analyze the surface changes in pre-oxidized MPs. Unfortunately, no diffraction peaks of MnO_2 were observed by XRD (Fig. S2), which is probably due to the amorphous nature of the MnO_2 produced on the surface of the microplastics, which was not crystalline or had a low content, resulting in inconspicuous diffraction peaks.

XPS analysis of PVC MPs with different oxidation methods was further carried out, and the XPS spectra of PVC MPs treated with $KMnO_4$ and UV/$KMnO_4$ oxidation methods at different pH were shown in Fig. 1. According to the spectra in Fig. 1a, it can be known that the O 1s spectra intensity of PVC MPs increased after $KMnO_4$ treatment. But the intensity was still weaker. After deconvolution, three characteristic peaks representing O–C, O=C, and O–Mn bonds were found in Fig. 1b, indicating that oxidation and the formation of manganese oxides (MnO_2) occurred on the surface of PVC MPs. As can be seen from Fig. 1c that the pH value also affected the degree of oxidation. The oxidation reaction of $KMnO_4$ is different under acidic and basic conditions, that is, the oxidation efficiency of potassium permanganate is higher under acidic conditions (Eq. (1)), while the formation of MnO_2 is enhanced under neutral and alkaline (Eqs. (2) and (3)). This conclusion was confirmed by the XPS results, which found the dominant role of the O–C peak during acid oxidation and the elevation of the O–Mn peak under neutral and alkaline conditions, suggesting that MnO_2 production may play an important role in the change of the surface of PVC MPs.

$$MnO_4^- + 8H^+ + 5e^- \rightarrow Mn^{2+} + 4H_2O\,(pH < 3.5) \quad (1)$$

$$MnO_4^- + 2H_2O + 3e^- \rightarrow MnO_2(s) + 4OH^-\,(pH\,3.5–12.0) \quad (2)$$

$$MnO_4^- + e^- \rightarrow MnO_4^{2-}\,(pH > 12.0) \quad (3)$$

It can be observed that the O–Mn peaks of the UV/$KMnO_4$ composite treatment were significantly higher than that of single $KMnO_4$ oxidation treatment under neutral and alkaline conditions in Fig. 1(d, e, f). This result indicated that the composite oxidation was able to intensify the oxidation on the surface of the PVC MPs, which can also be supported by

SEM results. For the pristine PVC MPs, no Mn 2p peak was observed in the XPS spectra, but its intensity increased after treatment with $KMnO_4$ as well as UV/$KMnO_4$ methods, which further demonstrated that oxidation and formation of MnO_2 occurred on the surface of the PVC MPs.

3.1.2. Surface hydrophobicity

Fig. S2a showed the contact angle of the PVC MPs treated with $KMnO_4$ single oxidation at different pH values. It can be seen that the contact angle of the pristine PVC MPs was 89.04°, showing a hydrophilic surface, but the contact angle of $KMnO_4$ treated MPs showed a decreasing trend, indicating that the surface tended to be hydrophilic. In addition, it was found that the pH value affected the degree of contact angle reduction. As shown in Fig. S3a, the contact angle of PVC MPs decreased from 89.04° to 81.32° after $KMnO_4$ oxidation, indicating that the change of contact angle was more obvious under neutral and alkaline conditions. Based on the FTIR and XPS results, the $KMnO_4$-induced surface oxidation was relatively weak, so the decrease in contact angle might be caused by other reasons. According to the XPS results, MnO_2 nanoparticles may be attached to the surface of MPs, which could enhance the surface wettability and make the surface more hydrophilic. The effect of pH on the contact angle was also consistent with this speculation, that was the aggregation of MnO_2 particles on the surface which made it more hydrophilic under neutral and alkaline conditions.

Fig. S3b showed PVC MPs treated with UV/$KMnO_4$ composite oxidation. It was found that the contact angle of PVC MPs decreased from 89.04° to 68.05° respectively, indicating that the composite oxidation treatment could intensify the adhesion of MnO_2 particles. Thus, the wettability of the surface was improved and the contact angle changes more obviously, which was also confirmed by the XPS results.

3.1.3. Surface morphology

During the pre-oxidation process, it was observed that the color of PVC MPs showed a change. To further understand the changes in the surface morphology of MPs, PVC MPs before and after pre-oxidation were characterized by scanning electron microscopy (SEM). SEM images of the pristine PVC MPs display that its surface is rough with more cracks and pores in Fig. 2(a, b, c), which can provide more adsorption sites. Fig. 2(f, g, h) was the SEM images of PVC MPs treated with single $KMnO_4$ pre-oxidation under pH = 3. It can be found that the surface morphology of PVC MPs shows obvious changes, including particle adhesion and surface oxidative corrosion. Fine solid particles of different sizes and aggregation states adhered to the surface of the oxidized MPs. These phenomena could be attributed to the oxidation of $KMnO_4$ to produce MnO_2, which was adhered and bound to the surface of MPs, and this hypothesis was also confirmed by the energy dispersive spectroscopy images (Fig. 2d, i, o).

It was found that the change in pH also had an effect on MnO_2 adhesion, and more MnO_2 particles were observed under neutral and alkaline conditions, which was consistent with the XPS results. In neutral and alkaline conditions, the MnO_2 does not dissolve in water, or even form agglomerates and further aggregates into large solids on its surface. Fig. 2(k, l, m) showed the SEM images of PVC MPs oxidized with UV/$KMnO_4$ composite method, it can be seen that the surface became rougher and more MnO_2 particles were attached to the surface, indicating that the composite oxidation can intensify the oxidation of the surface. The same results can be obtained from the XPS results and the Mapping images. However, the shape and morphology of MPs changed little after single and composite oxidation, indicating that the oxidation only occurred on the PVC MPs surface. The SEM of $KMnO_4$ single oxidation and UV/$KMnO_4$ composite oxidation under pH = 7 and 11 were described in Fig. S4 in Supporting Information. To visualize the particles on the surface of the pre-oxidized MPs better, the AFM characterization analysis was carried out (Fig. S5). Based on the AFM morphology of MPs, the morphological characteristics of the MnO_2 particles on the surface of the pre-oxidized MPs can be observed. Pre-oxidized MPs have a large amount of granular MnO_2 on their surface and the composite oxidized MPs contain more than the single oxidized MPs, a result that is consistent with the XPS and SEM-Mapping results.

3.2. The sorption kinetics

The relationship between the effect of time on the adsorption of MG by PVC MPs before and after single pre-oxidation of $KMnO_4$ is shown in Fig. 3a. After pre-oxidation, the adsorption capacity of the MPs for MG increased greatly to 7.0 mg/g at pH = 7, 6.7 mg/g at pH = 11 and 6.3 mg/g at pH = 3. It was found that the adsorption process of MG on the three MPs showed a similar trend, and was mainly divided into three stages: the first 12 h of the reaction was a fast adsorption process, and its adsorption was followed by a slow adsorption stage for 36 h. The dynamic adsorption equilibrium was reached at 48 h. For UV/$KMnO_4$ composite oxidation, the adsorption influence relationship of MG on the PVC MPs was shown in Fig. 3d. The adsorption capacity was increased obviously, and it was 140.7 mg/g, 123.8 mg/g and 122.9 mg/g when pH = 7, pH = 11 and pH = 3, respectively. The adsorption process was mainly divided into three stages: The first 48 h of adsorption is a fast adsorption process, followed by a slow adsorption phase in the next 12 h. The dynamic adsorption equilibrium is basically reached at 70 h. The analysis is mainly caused by the fact that the composite pre-oxidation contained more MnO_2 nanoparticles than the single oxidation PVC MPs. The difference in adsorption capacity of pre-oxidation PVC MPs at different pH values may be due to the different content of MnO_2 particles contained on their surfaces, thus further indicating that the presence of MnO_2 nanoparticles on the surface of PVC MPs is the main reason for the increase adsorption capacity of MG.

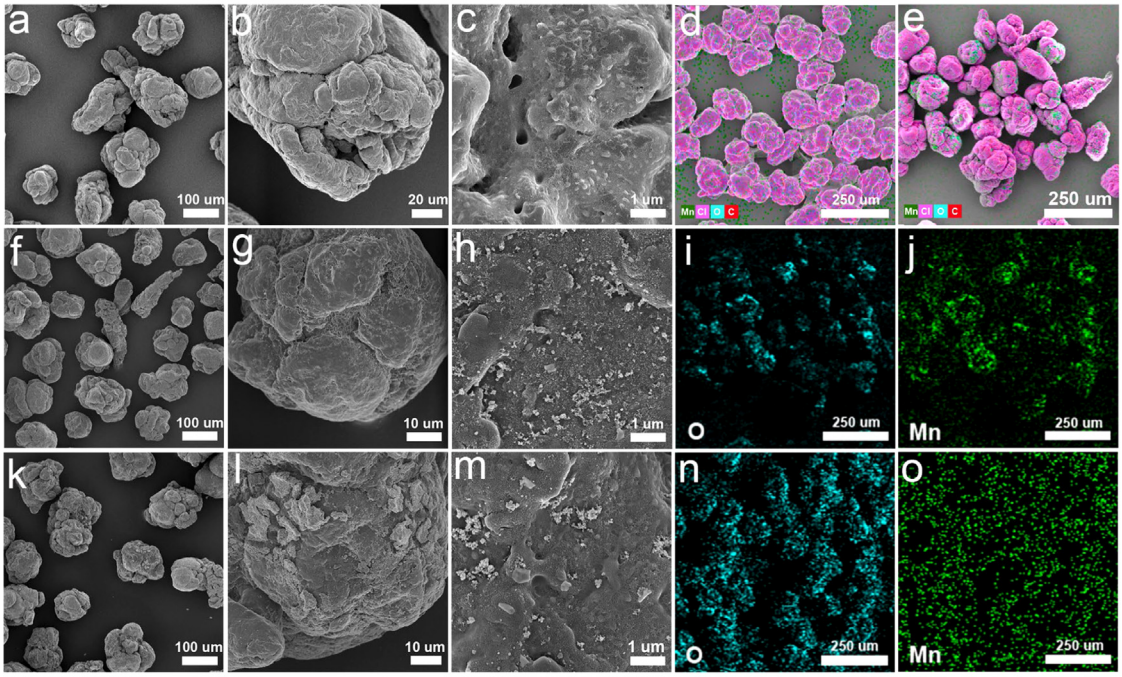

Fig. 2. Scanning electron microscope image of (a, b. c) pristine PVC MPs with different magnifications; (d) Energy dispersive spectroscope of PVC after $KMnO_4$ single oxidation under pH = 11; (e) Energy dispersive spectroscope of PVC after $KMnO_4$ composite oxidation under pH = 11; (f, g, h,) $KMnO_4$ single oxidation under pH = 3; (i, j) Energy dispersive spectroscope of O and Mn element after $KMnO_4$ single oxidation under pH = 11; (k, l, m) $KMnO_4$ composite oxidation under pH = 3; (n, o) Energy dispersive spectroscope of O and Mn element after $KMnO_4$ composite oxidation under pH = 11.. (For interpretation of the references to color in this figure legend, the reader is referred to the web version of this article.)

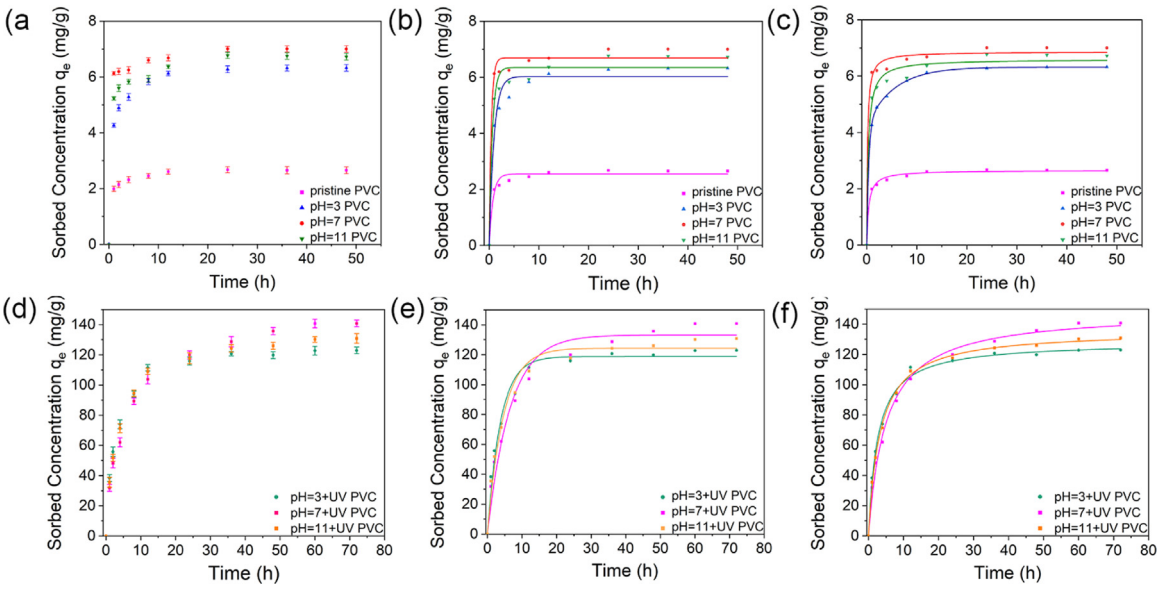

Fig. 3. (a, d) The effect of contact time on adsorption of MG on pristine PVC MPs, single and composite oxidation PVC MPs under pH = 3, 7, 11; (b, e) the sorption kinetics fitted by the pseudo-first-order model, (c, f) the sorption kinetics fitted by the pseudo-second-order model.

The efficiency-limiting steps and mechanism of MG adsorption on PVC MPs were studied by fitting the kinetic data with the pseudo-first-order and the pseudo-second-order models in Fig. 3(b-f). For the pristine MPs, the correlation coefficients (R^2) fitted by the different kinetic models are in Table 1, showing that the pseudo-first-order kinetic model fits the kinetic data better (R^2 > 0.967) than the pseudo-second-order kinetic model, which indicates that the adsorption process is

Table 1
Parameters of the kinetics models for sorption experimental data of MG on pristine, single and composite oxidation PVC MPs under pH = 3, 7, 11.

MPs	Pseudo-first order			Pseudo-second order		
	q_1 (mg/g)	K_1 (g/(mg h))	R^2	q_2 (mg/g)	K_2 (g/(mg h))	R^2
Pristine PVC	2.546 ± 0.062	1.3072 ±0.2160	0.967	2.656 ± 0.037	0.9118 ±0.1440	0.907
pH = 3 PVC	6.030 ± 0.155	1.0328 ±0.1563	0.966	6.335 ± 0.075	0.2865 ±0.0299	0.995
pH = 7 PVC	6.696 ± 0.1220	2.3247 ±0.5107	0.980	6.861 ± 0.099	0.9143 ±0.2599	0.991
pH = 11 PVC	6.351 ± 0.1643	1.5585 ±0.3108	0.962	6.598 ± 0.124	0.4772 ±0.1089	0.985
pH = 3+UV PVC	118.776 ± 2.584	0.2645 ±0.0261	0.978	128.233 ± 1.535	0.0031 ±0.0002	0.995
pH = 7+UV PVC	133.199 ± 3.991	0.1528 ±0.0183	0.969	148.589 ± 2.609	0.0013 ±0.0001	0.994
pH = 11+UV PVC	119.494 ± 2.451	0.3133 ±0.0303	0.979	128.121 ± 1.634	0.0036 ±0.0003	0.994

Table 2
Parameters of the isotherm models for sorption experimental data of MG on pristine, single oxidation and composite oxidation PVC MPs under pH = 3, 7, 11.

MPs	Langmuir model			Freundlich model		
	q_{max} (mg/g)	K_L (L/g)	R^2	K_F (L/g)	N	R^2
Pristine PVC	4.235 ± 0.774	0.0104 ±0.0054	0.964	0.1427 ± 0.052	1.2238 ±0.1568	0.948
pH = 3 PVC	14.263 ± 1.393	0.0133 ±0.0027	0.992	0.603 ± 0.086	0.8718 ±0.0459	0.977
pH = 7 PVC	13.326 ± 1.531	0.0167 ±0.0050	0.976	0.576 ± 0.173	1.3722 ±0.1618	0.953
pH = 11 PVC	14.409 ± 1.963	0.0105 ±0.0023	0.995	0.555 ± 0.132	1.2996 ±0.1170	0.971
pH = 3+UV PVC	213.679 ± 21.318	0.0297 ±0.0053	0.983	8.675 ± 0.968	1.1822 ±0.0411	0.991
pH = 7+UV PVC	215.352 ± 24.325	0.0362 ±0.0083	0.994	8.4055 ± 0.408	1.1762 ±0.0824	0.920
pH = 11+UV PVC	214.231 ± 23.251	0.0318 ±0.0059	0.991	8.616 ± 0.957	1.1925 ±0.0502	0.943

controlled by the diffusion step. As for the adsorption of MG by the $KMnO_4$ pre-oxidation PVC MPs, Table 1 shows that the pseudo-second kinetic model fits the adsorption kinetic data better with R^2 (0.986–0.995) than the pseudo-first kinetic model (0.963–0.980). This result indicates that the entire adsorption process is the result of multiple adsorption stages, such as liquid film diffusion on the microplastic surface, internal diffusion within microplastic particles, and chemical or physical adsorption at the adsorption site, and the main reason is the presence of surface MnO_2 nanoparticles. Moreover, for the adsorption kinetics of the composite pre-oxidation MPs, it was also found that the pseudo-second-order kinetic model fitted better with R^2 (0.994–0.995) than the pseudo-first-order kinetic model (0.968–0.995). The nano-MnO_2 was synthesized by a green method and found that it adsorbed 705 mg/g of MG, furthermore, the adsorption process fitted the pseudo-second-order kinetics model (Patra et al., 2022). The adsorption mechanism is mainly hydrogen bonding and π–π interaction, which is due to the π–π interaction between the aromatic ring π bond present in the malachite green molecule and Mn atom. There are empty d orbitals in the Mn atom, meanwhile, Mn can contribute electrons to π^* empty orbitals of the MG molecule, this type of bond formed between the Mn atom and MG molecule can act as a synergistic effect to improve the adsorption performance.

The interaction mechanism between PVC MPs and MG was further investigated by infrared spectroscopy for different oxidation methods. Fig. S1c shows the infrared spectra of MG adsorbed by pre-oxidation PVC MPs at different pH values. it can be seen that in all cases no band shift was observed, indicating that no chemical bond was formed between the PVC MPs and MG, and suggesting that chemisorption was not the main reason for the adsorption process (Liu et al. 2019; (Ma et al., 2019)); The same result can be observed in Fig. S1d, which indicates that physical adsorption plays a main role in the adsorption of MG by the PVC MPs after UV/$KMnO_4$ composite oxidation.

3.3. The sorption isotherm

The adsorption isotherms can reveal the equilibrium state of the adsorbate in solution and adsorbent, thus further elucidating the occurrence of the adsorption mechanism. Fig. 4(a, b, c) shows the adsorption isotherms of MG on the pristine, pH = 3 and pH = 3+UV PVC MPs, respectively. It can be seen that the adsorption capacity increases with the equilibrium concentration increased from 5 to 50 mg/L, while the slope of the corresponding curve gradually decreases. The adsorption of MG by PVC MPs is a process in which MG migrates from the aqueous solution to the solid surface of PVC MPs, when the adsorption sites on the surface of MPs are saturated, the adsorption will tend to equilibrium. (The results for pH = 7, pH = 11 PVC MPs; pH = 7 +UV and pH = 11+UV PVC MPs can be seen in Fig. S6 in SI.)

To further understand the adsorption mechanism, the adsorption data of MG on PVC MPs were fitted with Langmuir and Freundlich models, respectively, and the fitting results and isothermal parameters are shown in Fig. 4(d, e, f) and Table 2. By comparing R^2 values, it can be observed that the R^2 values calculated by the Langmuir model (0.964–0.995) were higher than those calculated by the Freundlich model (0.920–0.971) both the pristine and pre-oxidation PVC MPs. Such results indicated that the Langmuir model is more suitable for simulating MG adsorption than the Freundlich model. Langmuir isotherm adsorption refers to the adsorption of a single molecular layer with the same affinity for all sites to the adsorbent. The finding is consistent with MG adsorption on AC from the work (Qu et al., 2019). Thus, It indicates that the adsorption behavior of MG on PVC MPs is most likely monolayer and the adsorbent has a homogeneous distribution of active sites.

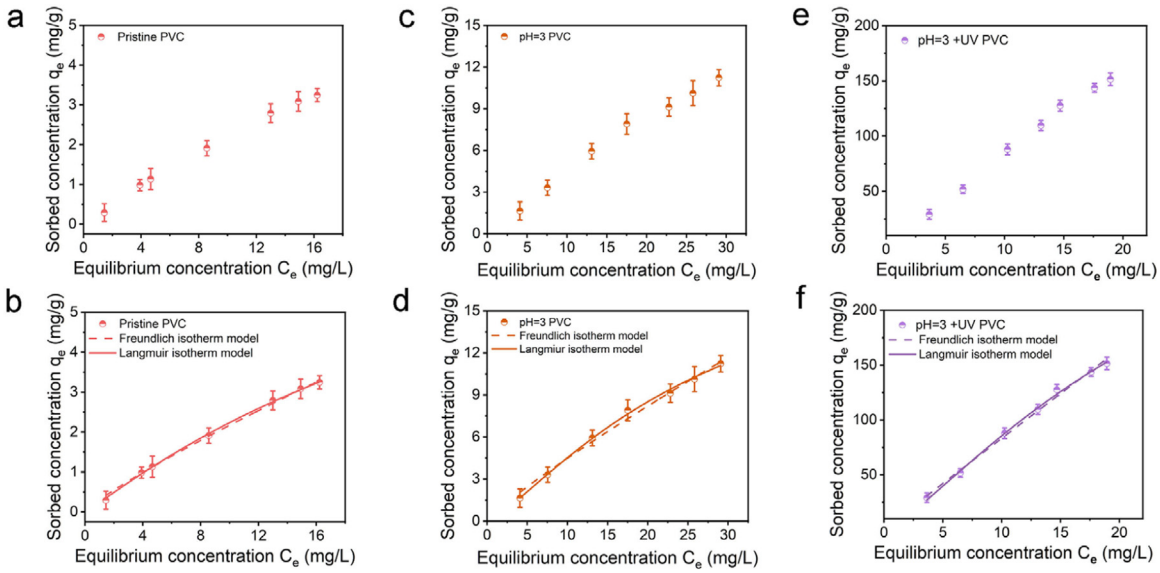

Fig. 4. (a, c, e) The effect of equilibrium concentration on adsorption of MG for pristine, pH = 3, pH = 3+UV PVC MPs; (b, d, f) The fitting graphs of adsorption isotherms models for pristine, pH = 3 and pH = 3 +UV PVC MPs, respectively.

3.4. The influence of pH and salinity

It was shown that MG is a cationic substance, and the electrostatic adsorption under alkaline and neutral conditions is more favorable to the adsorption process. The pH value of the MG solution is an important factor affecting the adsorption capacity of the adsorbent, so it is crucial to study the effect of pH on the adsorption of MG for PVC MPs. Fig. 5(a, b) shows the adsorption capacity of PVC MPs by single $KMnO_4$ and UV/$KMnO_4$ composite oxidation at different pH conditions, respectively. It can be known that the adsorption capacity of MG by both single and composite PVC MPs increased with the increase of solution pH values. The studied pH value range was from 2 to 7, where higher pH values led to the change of the dye from the green color to the colorless form, As a result, the UV device cannot detect the colorless dye (Kadhom et al., 2022). From Fig. 5(a, b), The adsorption capacity was the lowest at pH = 3 due to the competition for the same adsorption sites on the PVC MPs. Also, protonation at low pH produces strong electrostatic repulsions resulting in low adsorption capacity and tended to increase with increasing pH (Gautam et al., 2018). By the time the pH increases to 7, the adsorption capacity has reached the maximum. In acidic media, MG is a cationic substance, and the entry of protons can enhance the positive charge of the MG. In other words, PVC MPs are positively charged at lower pH solutions and negatively charged at higher pH solutions. Therefore, the attraction between the MG and the PVC MPs may occur and its intensity increases with the increase of charge difference.

With the migration of MPs from the freshwater environment to the marine environment, the salinity of water bodies usually increases from 5 to 50‰, and the change of salinity is important for the environmental behavior and attribution of pollutants in water bodies. Gradient NaCl solution was used to simulate the salinity environment of rivers, estuaries and oceans. Fig. 5(c, d) shows the adsorption of pre-oxidation PVC MPs by $KMnO_4$ and UV/$KMnO_4$ under different salinity conditions, respectively. It can be found that the adsorption of MG by PVC MPs increased with the increase of solution salinity, MG dissolved in water is in a cationic state and ionized in an aqueous solution to produce catatonically charged colored ions. This is mainly due to the dimerization of the dye in the solution, the high ionic strength promotes the aggregation of dyes and increases the adsorption on the surface of MPs (German-Heins and Flury, 2000). MPs in different experiments may have different properties, which are closely related to the polymer fabrication process. Even if MPs are of the same type, their properties such as crystallinity and specific surface area may be different, which may affect the adsorption behavior of pollutants. In general, the influence of salinity on adsorption may depend on the type of pollutants and MPs.

3.5. Desorption kinetics of MG from pristine and pre-oxidation PVC MPs

Desorption kinetics of pristine PVC, $KMnO_4$ pre-oxidation and UV/$KMnO_4$ composite oxidation MPs were studied in ultrapure water (pH = 7.2), simulated seawater, gastric fluid (pH = 2) and intestinal fluid (pH = 7). Gastric and intestinal fluids temperatures were maintained at 18 °C and 37 °C to simulate cold and warm blood organisms. Fig. 6a represents the desorption curves of pristine PVC MPs under the six simulated conditions, and it can be seen that pristine PVC MPs loaded with MG were desorbed at a faster efficiency within the first 10 h under all six desorption conditions, after that the

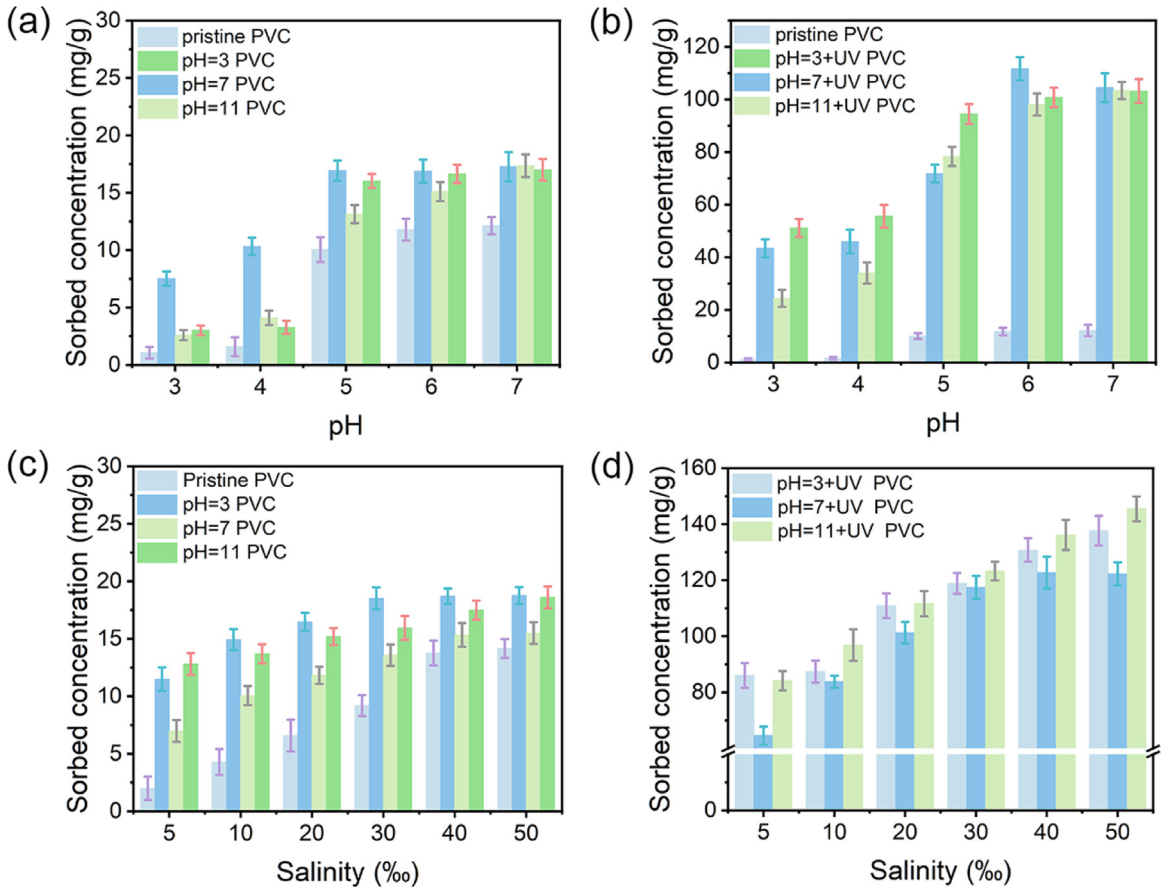

Fig. 5. The influences of (a, c) pH and (b, d) salinity on adsorption of MG for pristine, single oxidation and composite oxidation PVC MPs.. (For interpretation of the references to color in this figure legend, the reader is referred to the web version of this article.)

desorption efficiency was slower. The fast desorption phase was completed within 10 h, while the slow desorption phase lasted for months to years. Since the limited actual digestion time of marine organisms (ranging from hours to days), the fast desorption phase is more important for assessing the desorption behavior of MG in the simulated gastrointestinal fluids.

As can be seen in Fig. 6a, the high desorption capacity of the pristine PVC MPs in the gastric fluid was 3.8 mg/g, and the desorption efficiency was 60.0%, which may be due to the acidic conditions of the gastric fluid can promote the desorption of MG. When the temperature was increased to 37 °C, the desorption capacity increased to 4.0 mg/g and the desorption efficiency was 81.4%, indicating that high temperature could enhance the MG desorption in gastric fluid. The desorption capacity in the intestinal fluid was 2.5 mg/g and the desorption efficiency was 52.4%, moreover, the desorption capacity and desorption efficiency increased to 2.9 mg/g and 76.6% with the increase in temperature, respectively. This implies that once organisms ingest MG adsorbed by PVC MPs, there is a high probability that MG will be transferred from the surface of PVC MPs to the gastrointestinal fluids. The migration of contaminants to the organism becomes more pronounced as the ambient temperature increases, and this effect is more obvious for cold-blooded animals because their body temperature depends on the ambient temperature. The desorption in pure water was 2.1 mg/g with a desorption efficiency of 43.8%, while the desorption in simulated seawater was lower at 0.3 mg/g with a desorption efficiency of 5.7%, which may be mainly due to the higher ion concentration in simulated seawater will inhibit the desorption of the MG.

Fig. 6b shows the desorption curves of MG adsorbed by single pre-oxidation PVC MPs at pH = 3. The desorption efficiency of MG-loaded pre-oxidation PVC MPs was generally slower than the pristine PVC MPs under the six desorption conditions. The desorption efficiency basically reached the maximum at 40 h, after that the desorption efficiency was all slower. Fig. 6(c, d) shows the desorption curves of MG adsorbed by single pre-oxidation MPs at pH = 7 and 11. From Fig. 7, The desorption capacity and desorption efficiency are in the following order: 37 °C intestinal fluid (2.0 mg/g; 17.2%) > 18 °C intestinal fluid (1.8 mg/g; 15.6%) > ultrapure water (1.4 mg/g; 12.1%) > 37 °C gastric fluid (0.8 mg/g; 6.6%) > 18 °C gastric fluid (0.7 mg/g; 5.7%) > simulated seawater (0.2 mg/g; 1.3%). It was found that the desorption efficiency of $KMnO_4$ pre-oxidation PVC MPs was lower than that of the pristine PVC MPs, indicating that the combination between

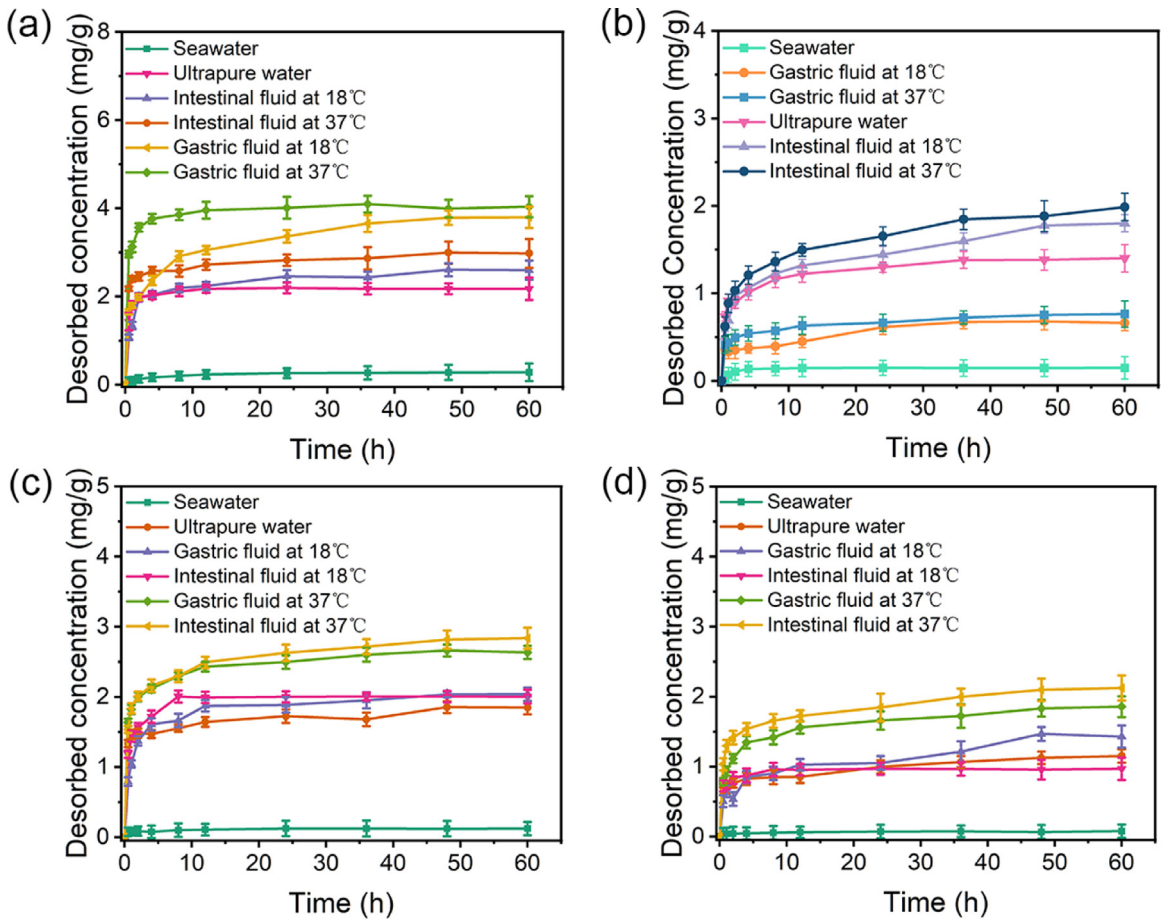

Fig. 6. Desorption time of MG on (a) pristine PVC MPs; (b) pH = 3 PVC MPs; (c) pH = 7 PVC MPs; (d) pH = 11 PVC MPs in simulated seawater, ultrapure water, gastric fluid at 18 °C, gastric fluid at 37 °C, intestinal fluid at 18 °C and intestinal fluid at 37 °C, respectively.

the pre-oxidation PVC MPs and MG was enhanced, which led to the difficulty in the desorption of MG. According to the previous adsorption kinetics, the adsorption increased after pre-oxidation due to the MnO_2 nanoparticles on the PVC MPs surface.

Therefore, the obvious decrease also may be caused by the better binding of surface MnO_2 nanoparticles to MG under the six simulated desorption conditions. Since the low desorption efficiency of MG by PVC MPs treated with UV/$KMnO_4$ composite oxidation, only 60 h desorption was carried out. The order of desorption capacity and desorption efficiency followed the order as: ultrapure water (1.3 mg/g; 0.8%) > 37 °C intestinal fluid (1.3 mg/g; 0.8%) > 18 °C intestinal fluid (1.1 mg/g; 0.7%) > 37 °C gastric fluid (0.8 mg/g; 0.5%) > 18 °C gastric fluid (0.6 mg/g; 0.4%) > simulated seawater (0.1 mg/g; 0.1%). Although the desorption capacity was similar to that of pre-oxidation PVC MPs at pH = 3, the desorption efficiency was generally lower. The main reason may be that there are more nano MnO_2 particles on the surface of the composite pre-oxidation PVC MPs than those of single oxidation, which leads to low desorption efficiency. The desorption efficiency of MG under various desorption conditions for pristine, pH = 7, pH = 7+UV, pH =11 and pH = 11+UV PVC MPs can be seen in Fig. (S7a, b) in SI.

3.6. Analysis of the adsorption mechanism of MG from pre-oxidation PVC MPs

To further verify the large adsorption capacity of pre-oxidation PVC MPs is mainly caused by the presence of MnO_2 particles on the surface, verification experiments were conducted. Herein, the PVC MPs after single and composite pre-oxidation were dissolved by sonication with sodium sulfite solution. it was found that brown pre-oxidation PVC MPs turned white. In addition, the surface MnO_2 particles were found to disappear by SEM results in Fig. S8.

The comparison experiments of process PVC MPs and single UV oxidation were also carried out. As we can see from Fig. S9 that the adsorption capacity decreased significantly for process PVC MPs. For example, The adsorption capacity of composite pre-oxidation pH = 3+UV PVC MPs was 123.0 mg/g, while the adsorption capacity changed to 2.4 mg/g

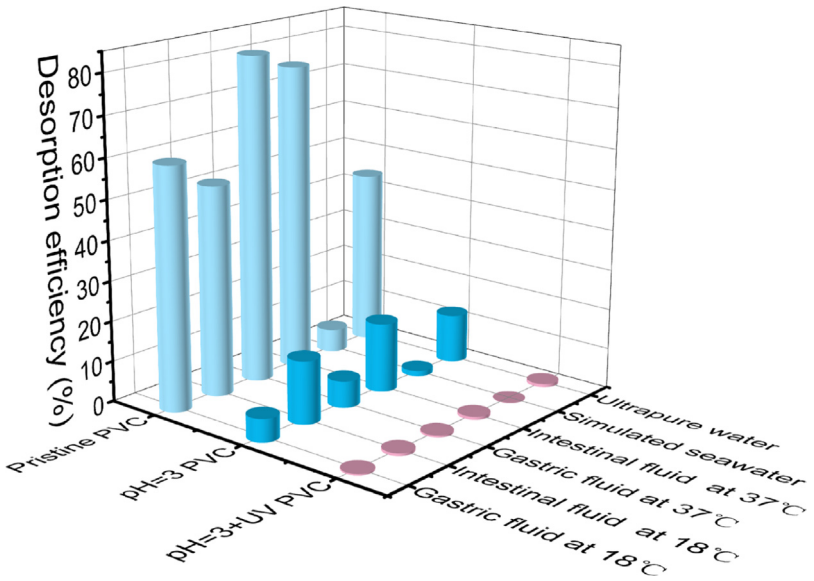

Fig. 7. Desorption efficiency of MG under various desorption conditions for pristine, pH = 3 and pH = 3+UV PVC MPs.

when processed. The adsorption capacity of the pristine PVC MPs was 0.6 mg/g but increased to 1.1 mg/g after the single UV oxidation. This indicates that the UV-oxidation PVC MPs also affect the adsorption of MG. This further illustrates the important role of MnO_2 on the surface of MPs in the adsorption process.

4. Conclusion

In this study, Polyvinyl chloride (PVC) MPs were treated by single and composite pre-oxidation with different pH values. $KMnO_4$ pre-oxidation can increase the hydrophilicity and adsorption capacity of MG on PVC MPs. Moreover, the adhesion of nano-MnO_2 particles on the surface of MPs was found to be the main factor by XPS and SEM-Mapping. Through adsorption experiments, the adsorption of MG by MPs with different oxidation methods was investigated, and the effects of pH and salinity on the adsorption were explored. Finally, the desorption behaviors were studied under different simulated conditions. These results indicate that there is a high potential that PVC MPs can transfer the surface of MG to the gastrointestinal fluids once the organisms ingest the MG-loaded PVC MPs.

CRediT authorship contribution statement

Kefu Wang: Conceptualization, Methodology, Validation, Formal analysis, Investigation, Data curation, Writing – original draft, Writing – review & editing, Visualization. **Kangkang Wang:** Validation, Formal analysis, Writing – review & editing. **Yaoyao Chen:** Software, Data analysis, Writing – review & editing. **Siqi Liang:** Investigation, Formal analysis. **Changyan Guo:** Methodology, Resources, Investigation, Formal analysis, Writing – review & editing, Visualization. **Wei Wang:** Project administration, Funding acquisition, Writing – review & editing. **Jide Wang:** Writing – review & editing, Supervision, Project administration, Funding acquisition.

Declaration of competing interest

The authors declare that they have no known competing financial interests or personal relationships that could have appeared to influence the work reported in this paper.

Data availability

Data will be made available on request.

Acknowledgments

This research was financially supported by the National Natural Science Foundation of China (Grant No. 32061133005) and the Research Council of Norway (RCN, project 320456).

Appendix A. Supplementary data

Supplementary material related to this article can be found online at https://doi.org/10.1016/j.eti.2023.103138.

References

Ahmed, R., et al., 2022. Critical review of microplastics removal from the environment. Chemosphere 293, 133557.
Bakir, A., et al., 2014. Enhanced desorption of persistent organic pollutants from microplastics under simulated physiological conditions. Environ. Pollut. 185, 16–23.
Bhagat, J., et al., 2021. Toxicological interactions of microplastics/nanoplastics and environmental contaminants: Current knowledge and future perspectives. J. Hazard. Mater. 405, 123913.
Cai, L., et al., 2018. Observation of the degradation of three types of plastic pellets exposed to UV irradiation in three different environments. Sci. Total Environ. 628–629, 740–747.
Coffin, S., et al., 2019a. Fish and seabird gut conditions enhance desorption of estrogenic chemicals from commonly-ingested plastic items. Environ. Sci. Technol. 53, 4588–4599.
Coffin, S., et al., 2019b. Simulated digestion of polystyrene foam enhances desorption of diethylhexyl phthalate (DEHP) and In vitro estrogenic activity in a size-dependent manner. Environ. Pollut. 246, 452–462.
Crini, G., 2006. Non-conventional low-cost adsorbents for dye removal: a review. Bioresour. Technol. 97, 1061–1085.
Dong, H., et al., 2021. Interactions of microplastics and antibiotic resistance genes and their effects on the aquaculture environments. J. Hazard. Mater. 403, 123961.
Egessa, R., et al., 2020. Microplastic pollution in surface water of Lake Victoria. Sci Total Environ 741, 140201.
Ferreira, A.M., et al., 2014. Complete removal of textile dyes from aqueous media using ionic-liquid-based aqueous two-phase systems. Sep. Purif. Technol. 128, 58–66.
Freeman, S., et al., 2020. Between source and sea: The role of wastewater treatment in reducing marine microplastics. J. Environ. Manag. 266, 110642.
Fu, W., et al., 2020. Separation, characterization and identification of microplastics and nanoplastics in the environment. Sci. Total Environ. 721, 137561.
Gautam, D., et al., 2018. A new hemicellulose-based adsorbent for malachite green. J. Environ. Chem. Eng. 6, 3889–3897.
German-Heins, J., Flury, M., 2000. Sorption of brilliant blue FCF in soils as affected by pH and ionic strength. Geoderma 97, 87–101.
Godoy, V., et al., 2020. Microplastics as vectors of chromium and lead during dynamic simulation of the human gastrointestinal tract. Sustainability 12.
Guo, X., et al., 2019. Sorption of sulfamethoxazole onto six types of microplastics. Chemosphere 228, 300–308.
Guo, H., et al., 2020. Leaching of brominated flame retardants (BFRs) from BFRs-incorporated plastics in digestive fluids and the influence of bird diets. J. Hazard. Mater. 393, 122397.
Holmes, L.A., et al., 2020. In vitro avian bioaccessibility of metals adsorbed to microplastic pellets. Environ. Pollut. 261, 114107.
Huffer, T., et al., 2018. Sorption of organic compounds by aged polystyrene microplastic particles. Environ. Pollut. 236, 218–225.
Jeong, C.B., et al., 2016. Microplastic size-dependent toxicity, oxidative stress induction, and p-JNK and p-p38 activation in the monogonont rotifer (Brachionus koreanus). Environ. Sci. Technol. 50, 8849–8857.
Jian, M., et al., 2020. Occurrence and distribution of microplastics in China's largest freshwater lake system. Chemosphere 261, 128186.
Jiang, J., et al., 2020. Investigation and fate of microplastics in wastewater and sludge filter cake from a wastewater treatment plant in China. Sci. Total Environ. 746, 141378.
Jin, Y., et al., 2018. Polystyrene microplastics induce microbiota dysbiosis and inflammation in the gut of adult zebrafish. Environ. Pollut. 235, 322–329.
Kadhom, M., et al., 2022. Performance of 2D MXene as an adsorbent for malachite green removal. Chemosphere 290, 133256.
Kelly, A., et al., 2020. Microplastic contamination in East Antarctic sea ice. Mar. Pollut. Bull. 154, 111130.
Lee, H., et al., 2019. Estimating microplastic-bound intake of hydrophobic organic chemicals by fish using measured desorption rates to artificial gut fluid. Sci. Total Environ. 651, 162–170.
Leslie, H.A., et al., 2017. Microplastics en route: Field measurements in the Dutch river delta and Amsterdam canals, wastewater treatment plants, North Sea sediments and biota. Environ. Int. 101, 133–142.
Li, L., et al., 2014. Kinetics of cell inactivation, toxin release, and degradation during permanganation of Microcystis aeruginosa. Environ. Sci. Technol. 48, 2885–2892.
Li, J., et al., 2018. Microplastics in freshwater systems: A review on occurrence, environmental effects, and methods for microplastics detection. Water Res. 137, 362–374.
Li, Y., et al., 2022. Adsorption behaviour of microplastics on the heavy metal Cr(VI) before and after ageing. Chemosphere 302, 134865.
Liao, Y.L., Yang, J.Y., 2020. Microplastic serves as a potential vector for Cr in an in-vitro human digestive model. Sci. Total Environ. 703, 134805.
Lin, T., et al., 2013. Role of pre-oxidation, using potassium permanganate, for mitigating membrane fouling by natural organic matter in an ultrafiltration system. Chem. Eng. J. 223, 487–496.
Liu, G., et al., 2019. Sorption behavior and mechanism of hydrophilic organic chemicals to virgin and aged microplastics in freshwater and seawater. Environ. Pollut. 246, 26–33.
Ma, J., et al., 2019. Effect of microplastic size on the adsorption behavior and mechanism of triclosan on polyvinyl chloride. Environ. Pollut. 254, 113104.
Mohamed Nor, N.H., Koelmans, A.A., 2019. Transfer of PCBs from microplastics under simulated gut fluid conditions is biphasic and reversible. Environ. Sci. Technol. 53, 1874–1883.
Nuelle, M.T., et al., 2014. A new analytical approach for monitoring microplastics in marine sediments. Environ. Pollut. 184, 161–169.
Ouyang, Z., et al., 2022. The photo-aging of polyvinyl chloride microplastics under different UV irradiations. Gondwana Res. 108, 72–80.
Patra, T., et al., 2022. Effect of calcination temperature on morphology and phase transformation of MnO2 nanoparticles: A step towards green synthesis for reactive dye adsorption. Chemosphere 288, 132472.
Payton, T.G., et al., 2020. Microplastic exposure to zooplankton at tidal fronts in Charleston Harbor, SC USA. Estuar. Coast. Shelf Sci. 232.
Qu, W., et al., 2019. Effect of properties of activated carbon on malachite green adsorption. Fuel 249, 45–53.
Rolsky, C., et al., 2020. Municipal sewage sludge as a source of microplastics in the environment. Curr. Opin. Environ. Sci. Health 14, 16–22.
Steinmetz, Z., et al., 2016. Plastic mulching in agriculture, Trading short-term agronomic benefits for long-term soil degradation? Sci. Total Environ. 550, 690–705.
Sun, S., et al., 2022. Effect of freeze-thaw cycle aging and high-temperature oxidation aging on the sorption of atrazine by microplastics. Environ. Pollut. 307, 119434.
Sussarellu, R., et al., 2016. Oyster reproduction is affected by exposure to polystyrene microplastics. Proc. Natl. Acad. Sci. USA 113, 2430–2435.
Tanaka, K., et al., 2015. Facilitated leaching of additive-derived PBDEs from plastic by seabirds' stomach oil and accumulation in tissues. Environ. Sci. Technol. 49, 11799–11807.
Wang, Z., et al., 2020. Occurrence and removal of microplastics in an advanced drinking water treatment plant (ADWTP). Sci. Total Environ. 700, 134520.
Zhang, Z., Chen, Y., 2020. Effects of microplastics on wastewater and sewage sludge treatment and their removal: A review. Chem. Eng. J. 382.